

Research Article

## Design and Analysis of Hollow Catenoidal Horn Profile for Ultrasonic Machining of Composite Materials

Muhammad Mubashir <sup>1,\*</sup> , Raza Mutahir <sup>1</sup> , Muhammad Shoaib Ur Rehman <sup>1</sup> 

<sup>1</sup> Department of Mechanical Engineering, University of Engineering and Technology Lahore, Lahore, 54000, Pakistan

\*Corresponding Author: Muhammad Mubashir, E-mail: mubashirmunir321@gmail.com

Article Info	Abstract
Article History	The composite materials Si/AlC, crystal quartz, and ceramic glass are becoming an important part of the present society in many engineering and non-engineering fields. Conventional methods available for machining these materials have many flaws due to which their application on large scale is restricted. A non-conventional process known as ultrasonic machining (USM), can be implemented for machining of these materials effectively. Anyhow machining efficiency of USM greatly depends upon its horn design and therefore in the present study a horn based on a catenoidal profile with aluminum and titanium material for USM was designed and developed by using solid works and ANSYS. Modal and harmonic analysis was done on the horn for computation of various parameters of interest such as resonant frequency, amplitude vibration and equivalent stresses. After the computation of the results, they were analyzed and compared with those available in the literature in terms of stresses and magnification factor for their validation comparison with literature, it was found that an aluminum catenoidal horn shows higher magnification with the least stress magnitude as compared to horns available in the literature and hence can be used in USM as a replacement for existing horns.
Received Apr 15, 2022	
Revised Jun 22, 2022	
Accepted Jun 01, 2022	
<b>Keywords</b>	
Catenoidal Horn	
Ultrasonic Machining	
Modal Analysis	
Harmonic Analysis	
Magnification Factor	



**Copyright:** © 2022 Muhammad Mubashir, Raza Mutahir and Muhammad Shoaib Ur Rehman. This article is an open-access article distributed under the terms and conditions of the Creative Commons Attribution (CC BY 4.0) license.

### 1. Introduction

The composite materials Si/AlC, crystal quartz, ceramic glass are becoming an important part of the present society in many engineering and non-engineering fields, such as aeronautical (advanced parts of engine and turbine), medical (for ultrasound and optic lenses), and aerospace (wings of jet engines), etc. because of their high strength with very low weight, low density, and high stability against chemical action [1-4]. Conventional methods available for machining these materials have many flaws of low processing efficiency, burr, high tool wear, etc. To overcome these defects, a non-conventional process known as ultrasonic machining (USM), can be used for machining of these materials effectively. In the USM tool vibrate at a frequency greater than audible frequency. A common frequency of operation of USM is more than 20 kHz. Generally, USM consists of a generator, transducer, horn, and tool as its main assembly. The

generator produces electrical signals of a small frequency magnitude of 40 Hz, these signals are transmitted to the transducer via transmission cables. Magneto strictive action of transducer converts electric signals into vibrations of low amplitude. This low amplitude requires amplification for performing machining of composites hence this amplification is achieved by using an element known as a mechanical horn. The basic setup of USM is shown in figure 1.

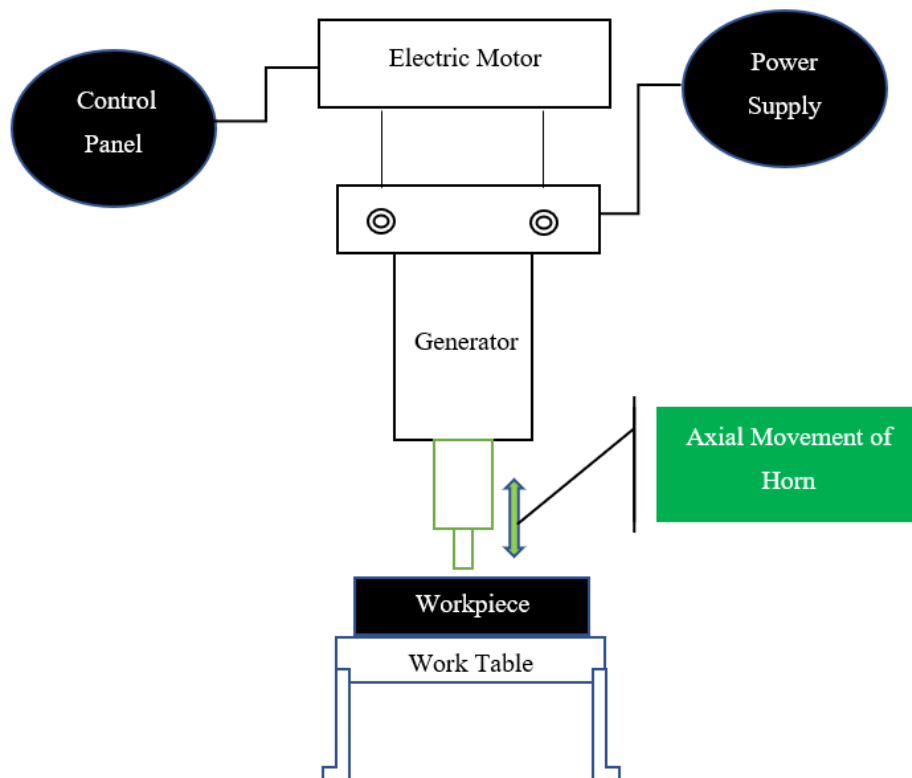


**Figure 1.** The basic setup of USM and its parts

A novel horn design by using 3rd order polynomial equation was developed and designed by Mughal et al [5]. They used the modal and harmonic analysis module of ANSYS in their analysis for evaluation of the performance of various horns (step, catenoidal, quadratic Bezier, cubic Bezier, Gaussian, etc.) available in the literature and compared their results with the novel horn. They recommend under the same operating conditions novel design of the horn shows high magnification of vibration with low stresses and can be used as a new horn for ultrasonic application.

Seah et al [6]. used three different simulation methods and performed modal analysis to the estimation of resonance frequency for their designed horns. They verified their results experimentally by manufacturing sonotrode designs based on simulation. They found both results are much similar to each other with

little error. They also compared conical and step horn profiles for USM and found later gives high amplification as compared to prior. Amin et al [7]. implemented the FEM technique using ANSYS and developed a compound horn profile with the shape of conical and step for USM. FEM-based ANSYS and Multiobjective functioning optimization were used by wang et al [8]. for the development of a new horn profile for high amplification achievement. He developed a cubic Bezier horn in his research and found that his designed bezier horn gives higher amplification as compared to the conventionally available horn. A profile of horn for USM based on some basic Webster and differential equations was prepared by Rosca et al [9]. They implemented their design horn in the mechanical ultrasound industry. Roy et al [10]. performed modal and harmonic analysis on the hollow exponential horn for estimation of various stresses. They used the ANSYS workbench for the computation of modal frequency, amplitude vibration, and various stresses for their designed horn. Based on their analysis they developed a profile that gives high amplification with low stresses as compared to previously existing horns.

Jagadish et al [11]. designed and developed a horn with exponentially decreasing rectangular cross-sectional area from transducer side to tool side. They performed modal and harmonic analysis for their horn and found their designed horn gives a higher amplification factor as compared to exponential and conical horns with low stresses. However, their designed horn shows 71% less amplification as compared to conventional step horn. A horn for equal channel press (ECP) process was developed by Naseri et al [12]. For achievement of resonant frequency, they performed modal analysis on horns of long length by using the finite element method (FEM). They also verified their results experimentally for showing the effectiveness of FEM. According to them for the best performance of the horn, all the parts of the machine must be operated with it at the correct resonance.

Rani et al [13]. developed horns to be used in ultrasonic welding (UW) based on thermoelastic analysis. They used mild steel, titanium, stainless steel, and aluminum as a material for their horns and found a horn made of titanium material that shows higher amplification and can be utilized in UW without failure due to dynamic loads. The performance of the stepped horn to be used in ultrasonic-assisted welding was analyzed by wang et al [14]. Raj et al. [15] used FEM for designing and optimization of quadratic and cubic Bezier ultrasonic horns for rotary ultrasonic machining system. In their study they compared the results of

both horns with each other in term of vibration amplification and stresses. They found cubic bezier horn shows better results as compared to quadratic horn in term of vibration and stress.

It is clear from the above literature review different researches have been conducted up to now regarding the design of horn for getting maximum amplification with low stresses magnitude at resonance. It can also be analyzed that horn designs of various shapes including cylindrical, exponential, stepped, conical, etc. have been done by different researchers for USM for achieving high material removal rate from the workpiece. All the profiles that were found analyzed by various researchers have solid cross sectional except the work done by Roy et al [10].

Furthermore, literature shows that the work for horn performance design based on a catenoidal profile with a circular hole at its tool end for USM using ANSYS and two different materials has not been done yet by any researcher. Hence, the main objective of this study is to analyze the design performance of a catenoidal horn profile with a circular hole for two different materials (aluminum and titanium). Therefore, in the present study, modal and harmonic analysis modules of ANSYS were used for the computation of axial amplification, stresses, and resonance frequencies of the horns. Computed results are then compared with literature for their validation and acceptance.

## 2. Materials and Methods

### 2.1 Mathematical Modeling and Assumptions

Following are the main assumptions regarding the mathematical modeling of present horn design,

- The material of the horn is isotropic, which means the material has the same properties along the length direction.
- Horn vibration is periodic motion which means it moves harmonically.

#### 2.1.1 Displacement Equation of Horn

An equation that describes the propagation of an axial wave through an ultrasonic horn of inconstant circular cross-sectional area is known as webster's equation [16-18] given below,

$$\frac{\partial^2 v(x,t)}{\partial x^2} + \frac{\partial^2 v(x,t)}{\partial x^2} \frac{\partial}{\partial x} \ln A(x) = \frac{1}{n^2} \frac{\partial^2 v(x,t)}{\partial t^2} \quad (1)$$

In the above equation (1),  $v(x, t)$  is the axial displacement of the ultrasonic horn with respect to its position and time,  $A(x)$  is the cross-sectional area of a horn as a function of its position along axial length

of the horn and  $n$  is the speed of waves with which it travels in any horn of given material it depends upon material density and elasticity and can be computed as follow,

$$n = \sqrt{E/\rho} \quad (2)$$

For a horn that exhibits periodic motion equation (1) can be transformed as follows [5],

$$\frac{\partial^2 v(x,t)}{\partial x^2} + \frac{\partial^2 v(x,t)}{\partial x^2} \frac{\partial}{\partial x} \ln A(x) = \frac{\omega^2}{n^2} \partial^2 v(x,t) \quad (3)$$

In the above equation ratio of rotational speed,  $\omega$  to axial speed  $n$  is known as the circular wave number of horn that remains constant for a given horn throughout its operating condition and hence replacing  $\frac{\omega^2}{n^2} = S^2$  in equation (3) gives,

$$\frac{\partial^2 v(x,t)}{\partial x^2} + \frac{\partial^2 v(x,t)}{\partial x^2} \frac{\partial}{\partial x} \ln A(x) = S^2 \partial^2 v(x,t) \quad (4)$$

The solution of the above equation gives displacement as a function of its position and time as given below (5).

$$v(x,t) = \frac{k_1 \sin Sx + k_2 \cos Sx}{\sqrt{A(x)}} \quad (5)$$

Above equation (5) is the final equation that can be used for the computation of displacement of the ultrasonic horn while  $k_1$  and  $k_2$  are the constants that can be computed using initial conditions for the given horn.

### 2.1.2 Stresses Equation of Horn

In a cylindrical coordinate ( $r - \theta - z$ ) system stresses on the horn can be computed by using the following equations [19],

$$\frac{\partial \sigma_r}{\partial r} + \frac{1}{r} \frac{\partial \tau_{r\theta}}{\partial \theta} + \frac{\partial \tau_{rz}}{\partial z} + \frac{\sigma_r - \sigma_\theta}{r} + B_r = \rho \frac{\partial^2 \mu_r}{\partial t^2} \quad (6)$$

$$\frac{\partial \tau_{r\theta}}{\partial r} + \frac{1}{r} \frac{\partial \sigma_\theta}{\partial \theta} + \frac{\partial \tau_{\theta z}}{\partial z} + \frac{2\tau_{r\theta}}{r} + B_\theta = \rho \frac{\partial^2 \mu_\theta}{\partial t^2} \quad (7)$$

$$\frac{\partial \tau_{rz}}{\partial r} + \frac{1}{r} \frac{\partial \tau_{\theta z}}{\partial \theta} + \frac{\partial \sigma_z}{\partial z} + \frac{\tau_{rz}}{r} + B_z = \rho \frac{\partial^2 \mu_z}{\partial t^2} \quad (8)$$

In above equations  $\sigma_r$ ,  $\sigma_z$  and  $\sigma_\theta$  are the radial, axial and circumferential stresses of the horn respectively. While  $\tau_{r\theta}$ ,  $\tau_{\theta z}$  and  $\tau_{rz}$  are the shear stresses acting on the ultrasonic horn in the respective plane and  $B_r$ ,  $B_z$  and  $B_\theta$  are the body force acting on the horn.

### 2.1.3 Magnification Factor (MF) of Horn

It is defined as the ratio of amplitude vibrations at the tool end to amplitude provided to the horn at the transducer end [20].

$$MF = \frac{\text{Vibration amplitude at tool end of horn}}{\text{Vibration amplitude at transducer end of horn}} \quad (9)$$

For efficient utilization of horn in USM magnitude of MF should be greater than 1.

### 2.2 Design of Horn

CAD modeling software package Solid works (SW) 2018 was used for the development and designing of the horn CAD model. Equation driven curve option of SW was used for sketching of catenoidal curve. The main equation on which the catenoidal curve is generated is given below [5, 8, 21],

$$y(x) = d \cosh \beta(x - l) \quad (10)$$

In the above equation (10)  $\beta$  is known as the ascent factor of the curve and computed by using boundary conditions as follows,

$$\beta = -\left(\frac{\cosh^{-1}\left(\frac{D}{d}\right)}{l}\right)$$

In the present study  $D = 40 \text{ mm}$  is the transducer side diameter of the catenoidal horn,  $d = 5 \text{ mm}$  is the tool side diameter of the catenoidal horn and  $l = 120.69 \text{ mm}$  is the total length of horn taken from reference [10] for making comparison easy. A 2D sketch based on the above dimensions for the catenoidal horn is shown in figure 2.

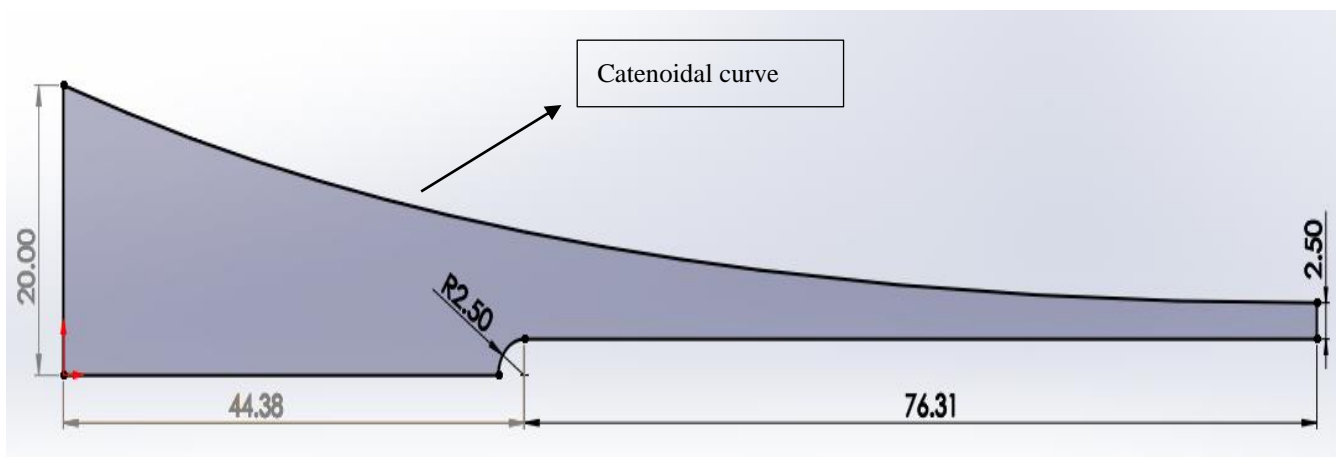


**Figure 2.** Detailed 2D sketch for catenoidal horn

### 2.2.1 Materials of Horn

In the present study, horn performance was evaluated by using two different materials aluminum alloy and titanium alloy. Their core properties required for the present analysis are listed in table 1.

**Table 1.** Material properties of aluminum and titanium alloy used for the analysis of catenoidal horn

Material	Density $\rho$ $kg. mm^{-3} \times 10^{-6}$	Elastic Modulus $E$ (GPa)	Poisson ratio $\nu$	Yield strength $\sigma_y$ (MPa)
Titanium Alloy	4.42	115	0.342	382
Aluminium Alloy	2.77	71.0	0.33	280

### 2.3 Modal Analysis

The CAD model was imported into ANSYS and modal analysis was performed on it for the determination of resonance frequency using ANSYS. Fixed support at the transducer end was used as a boundary condition for modal analysis in ANSYS. Mechanical default control mesh (solid 187 element) with a mesh size of 1mm was selected for the meshing purpose of the imported model in the present study. The total number of elements and nodes generated after completion of mesh was 17328 and 30254 respectively. Furthermore, the number of modes was set to 30 in the analysis setting of modal analysis.

### 2.4 Harmonic Analysis

The CAD model was imported into ANSYS and harmonic analysis was performed on it for the determination of axial amplification of amplitude, normal (axial) stress, shear stress, von mises stress, and circumferential stresses. 15  $\mu m$  initial amplitude at the transducer end was used as a boundary condition for harmonic analysis in ANSYS. Again, for this module same mesh control was chosen as given above in modal analysis. However, in the analysis setting mode superposition method with a frequency range of 21-25 kHz was used for the analysis of the results.

## 3. Results and Discussions

### 3.1 Modal Analysis Results

Based on the methodology discussed above the contour plot of resonant frequency for aluminum and titanium catenoidal horns is shown in Figures 3 and 4 respectively. From the figures resonant frequencies come up 34459 Hz and 34736 Hz respectively for aluminum and titanium catenoidal horns, as frequencies

of both horns are greater than 20,000 Hz which is one of the core requirements for the horn to be used in USM, hence both horns can be operated very effectively in an ultrasonic machine for machining of hard and brittle materials.

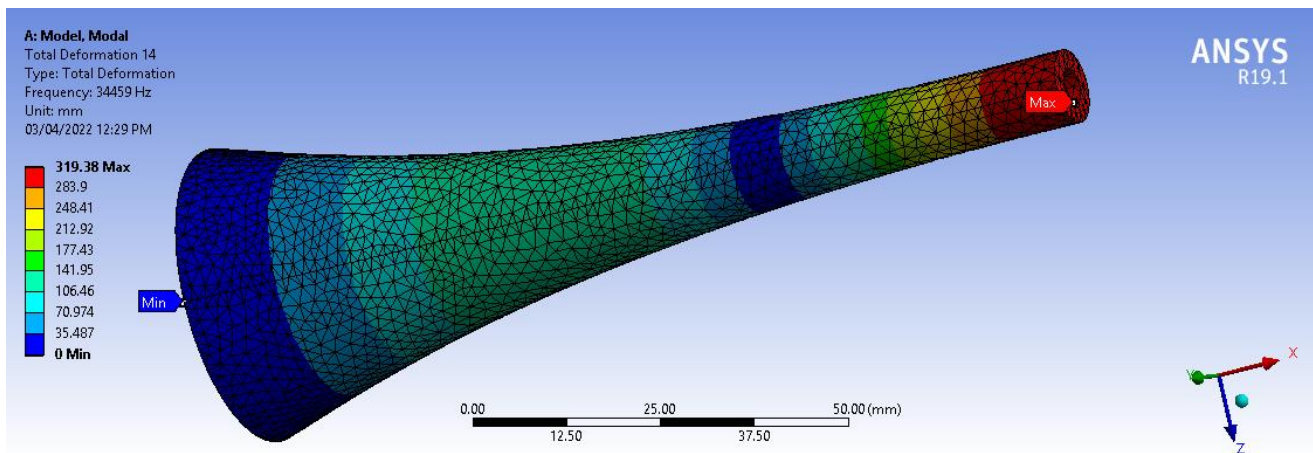


**Figure 3.** Resonant frequency result of aluminum horn corresponding to 2<sup>nd</sup> axial mode

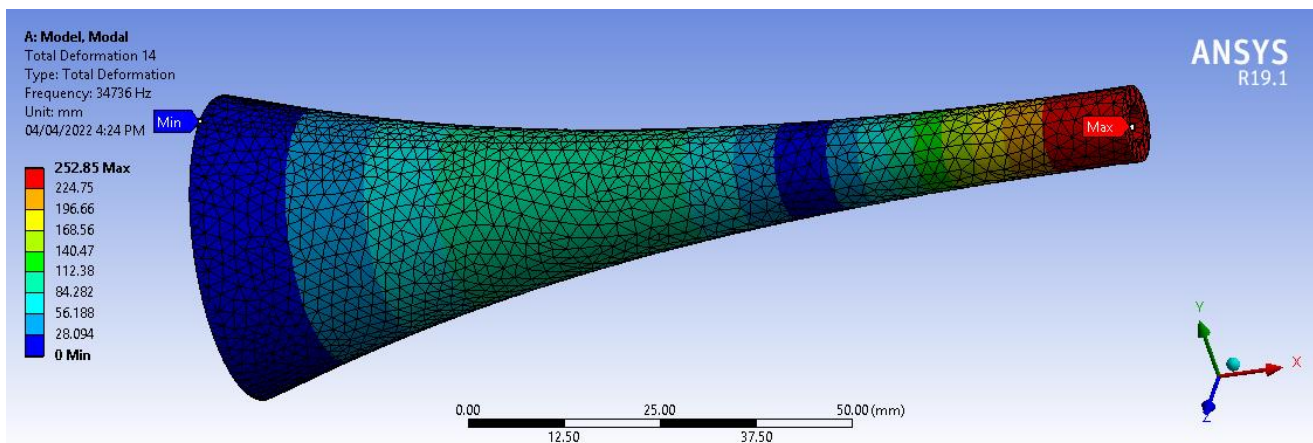


**Figure 4.** Resonant frequency result of titanium horn corresponding to 2<sup>nd</sup> axial mode

### 3.2 Harmonic Analysis Results

The results of vibration amplitude and corresponding equivalent stress along the axial length of both horns are shown in figures 5, 6, 7, and 8. From Figures 5 and 7 maximum amplitude vibration of 78.587  $\mu\text{m}$  and 79.745  $\mu\text{m}$  can be achieved at the tool end by implementing a catenoidal horn of aluminum and titanium materials respectively. From equation (10) corresponding M.F for aluminum and titanium catenoidal horns comes up to 5.23 and 5.32 respectively.



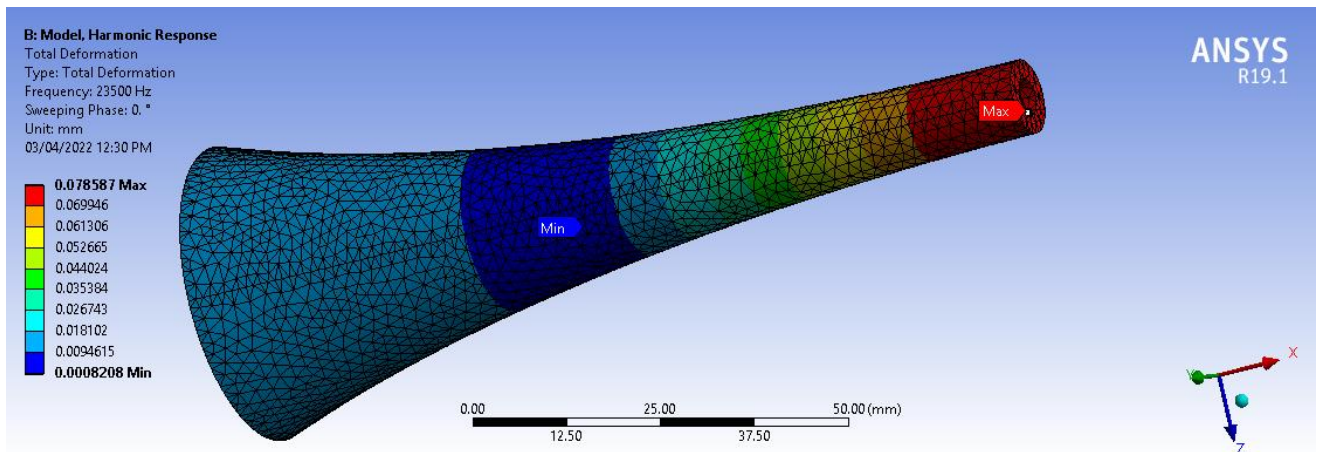


**Figure 5.** Variation of vibration amplitude along the axial length of aluminium catenoidal horn

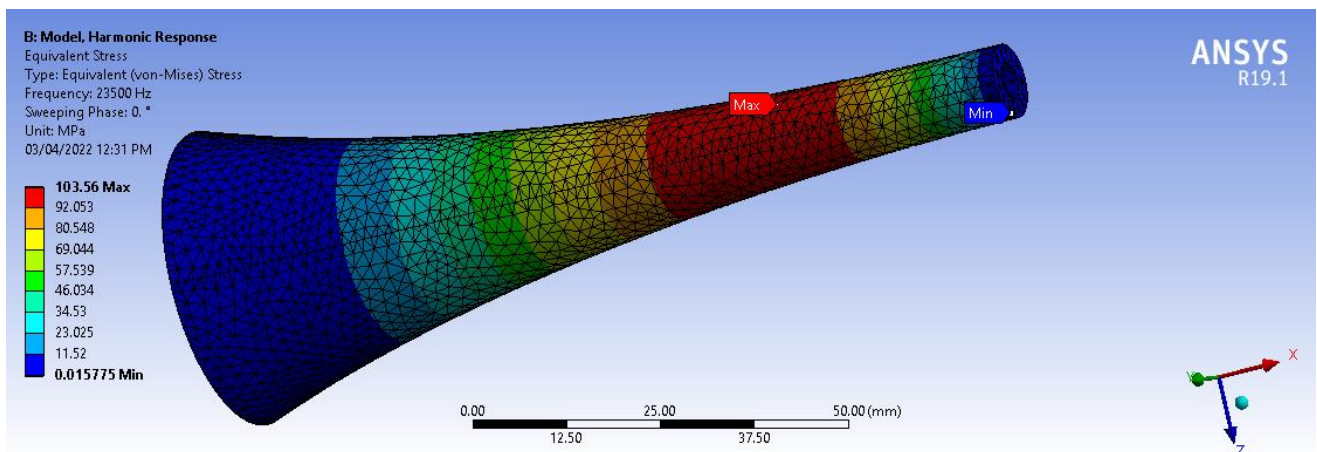


**Figure 6.** Variation of equivalent stress along the axial length of aluminum catenoidal horn

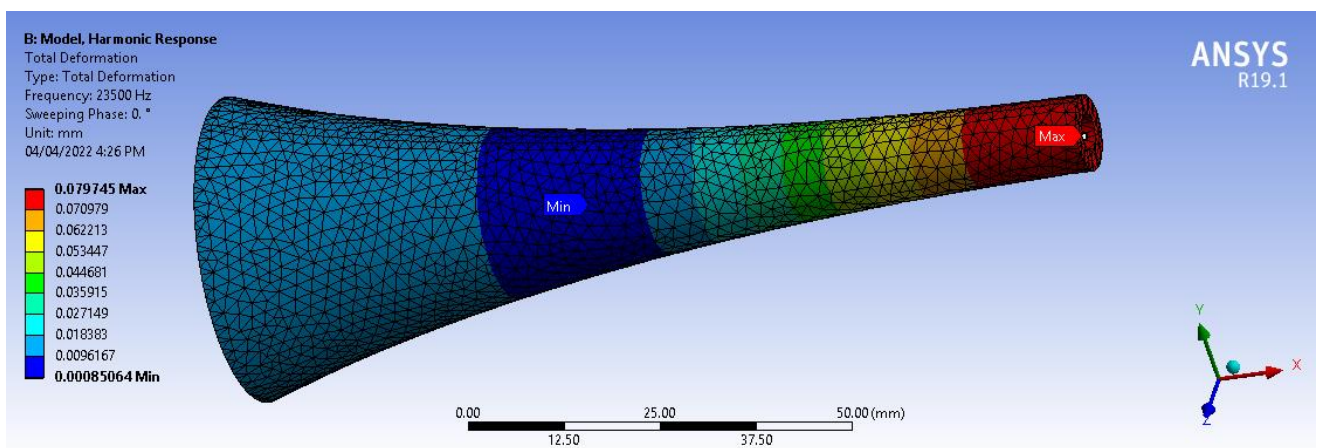


**Figure 7.** Variation of vibration amplitude along the axial length of titanium catenoidal horn

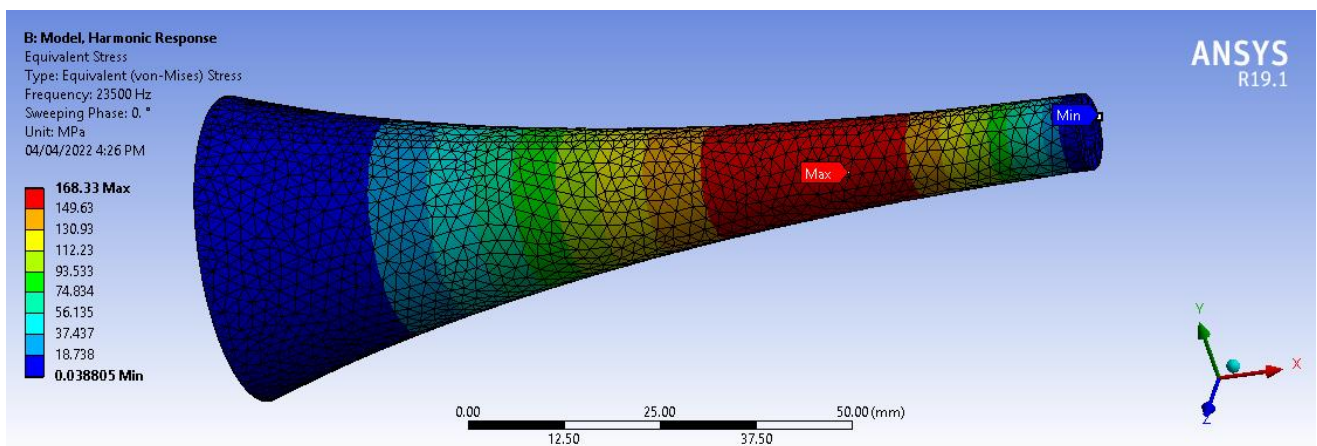


**Figure 8.** Variation of equivalent stress along the axial length of titanium catenoid horn

### 3.3 Validation of Results

The results of the present research are validated by making their comparison with the results of various horns available in literature in terms of their M.F and equivalent stress. A graphical comparison plot between the vibration amplitude of present aluminium and titanium catenoidal horn with the hollow exponential horn [10] of literature is shown in figure 9

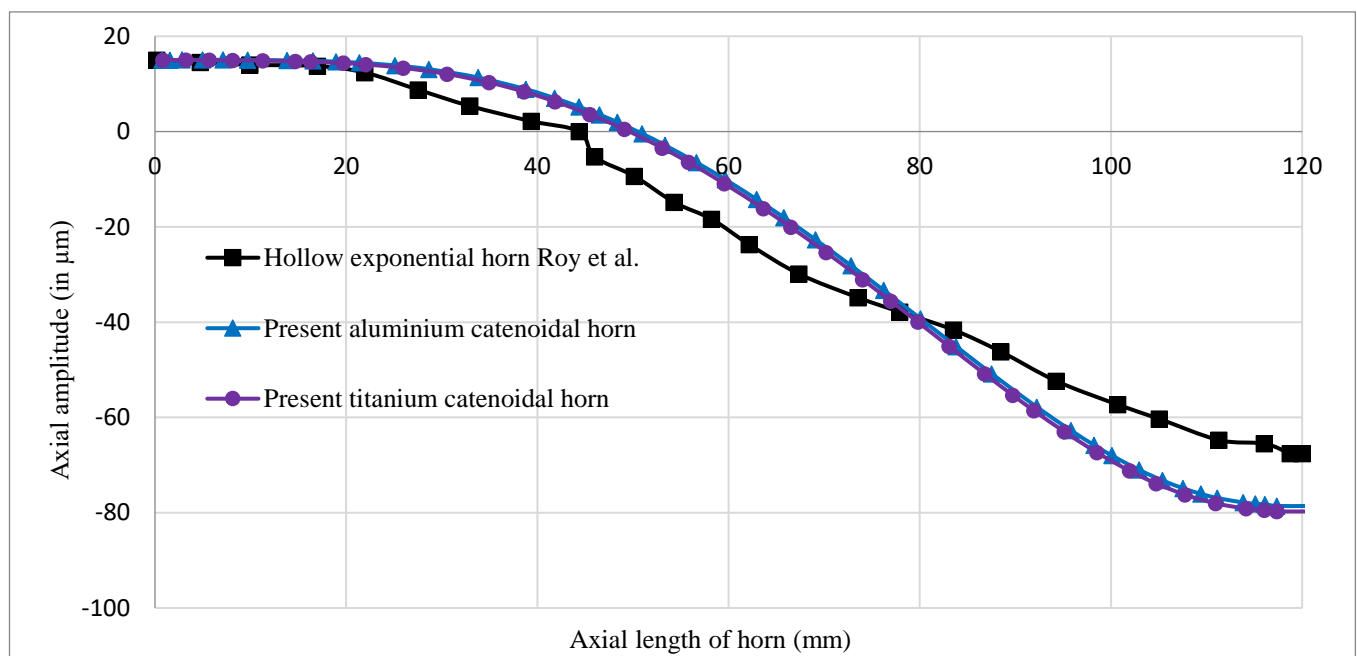


**Figure 9.** Amplitude variation of various horns

Refer to the same figure vibrational amplitude along the length of horn for presently designed aluminium and titanium horn is almost higher than hollow exponential horn. Maximum amplitude vibration

of 78.587  $\mu\text{m}$  and 79.745  $\mu\text{m}$  can be achieved at the tool end by implementing a catenoidal horn of aluminium and titanium materials respectively which is higher than the vibration amplitude (67.559  $\mu\text{m}$ ) achieved by the implementation of the exponential horn of the same end dimensions and conditions.

While at the same time, a graphical comparison plot of equivalent stress generated under identical input conditions within the present aluminium and titanium catenoidal horns and hollow exponential horn of literature is shown in figure 10. Refer to the same figure maximum equivalent stress developed in aluminium catenoidal, titanium catenoidal and hollow exponential horns are 103.56 MPa, 168.33 MPa, and 133.33 MPa. In terms of equivalent stress, and aluminium catenoidal horn shows less stress with higher M.F and can be accepted as a new design of horn. While titanium catenoidal shows higher stress as compared to hollow exponential horn available in the literature.

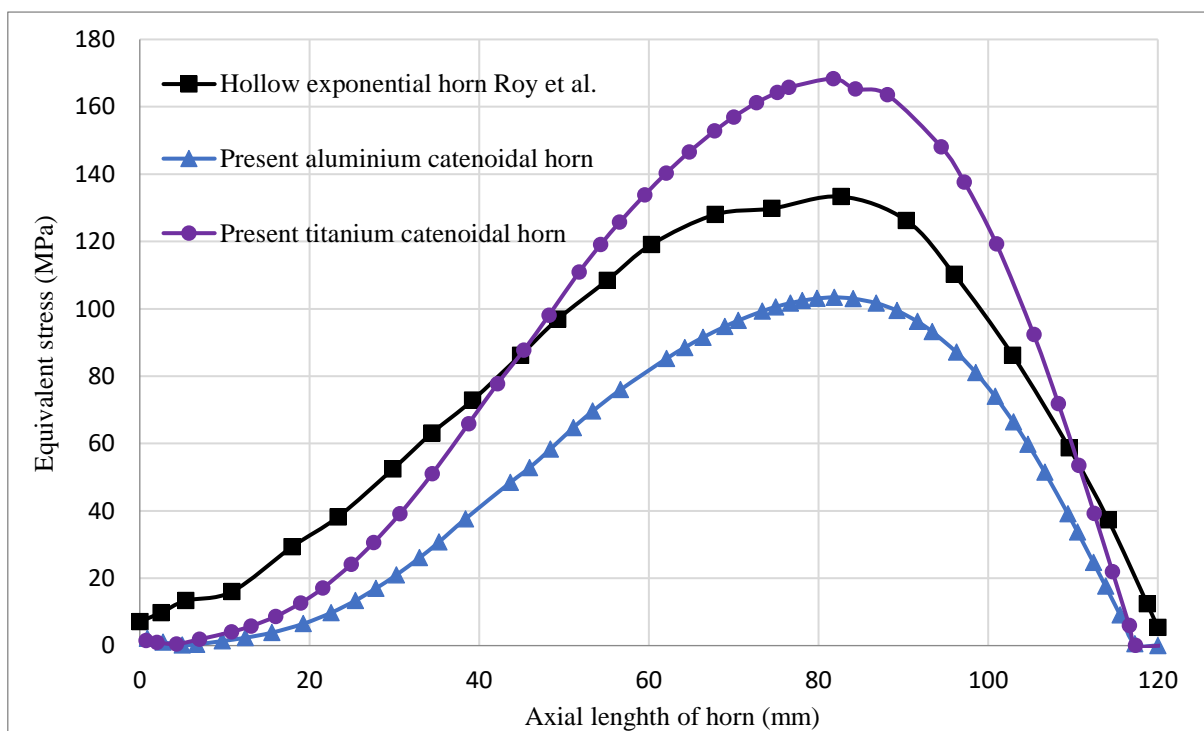


**Figure 10.** Equivalent stress variation of various horns

Although, the stress magnitude developed in titanium catenoidal profile is higher than hollow exponential but still lies within the yield limit (382 MPa) of material with higher M.F of 5.32 as compared to hollow exponential horn with M.F of 4.5 and hence this design can also be accepted and used as a replacement of existing design of horn in USM. Furthermore, making the validation of present results further stronger comparison of presently designed horns are also made with the horns developed by Amin et al [7].

in their research by using the CAD procedure method. A comparison and overall summary of various horns are shown in table 2.

**Table 2.** Comparison of aluminium and titanium catenoidal horns with other horns [7, 10]

Horn type	$r_2/r_1$	Equivalent stress	M.F
Step	4	Exceed yeild limit	16
Conical	4	188	3.39
Exponential	4	220	3.94
Hollow exponential	4	133.3	4.5
Titanium catenoidal	4	168.33	5.32
Aluminium catenoidal	4	103.56	5.23

Concerning table 2, if various horns of the same radius ratio are utilized for USM then it can be seen maximum M.F of 16 can be achieved by the implementation of the stepped horn. Although this M.F is very high but stresses generated within the horn exceeded the yield limit because of stress concentration encounters hence a stepped horn can not be used in USM. Referring to the same table 2, an aluminum catenoidal shows high MF with the least stresses as compared to hollow exponential, exponential, step, and conical horns profiles and hence is the safest design for the horn for USM.

#### 4. Various Stresses Plot

A plot for variation of core stresses such as axial, radial, shear, and circumferential stresses along the axial length of horn for presently designed titanium and aluminium catenoidal horns is shown in figures 11 and 12 respectively. For both horns magnitude variation in radial, shear and circumferential stresses are very small and remain very well below the yielding strength throughout the axial length of the horn hence both horns are safe against these stresses. The only prominent stress for both horns is axial stress which achieves the maximum magnitude of -103.56 MPa for aluminium and -168.33 MPa for titanium catenoidal horn. However, both these magnitude of axial stresses are less than the yield limit of material hence, lie within the acceptable range therefore horns are also safe against axial stress and can be used effectively in USM for machining of hard composite materials.

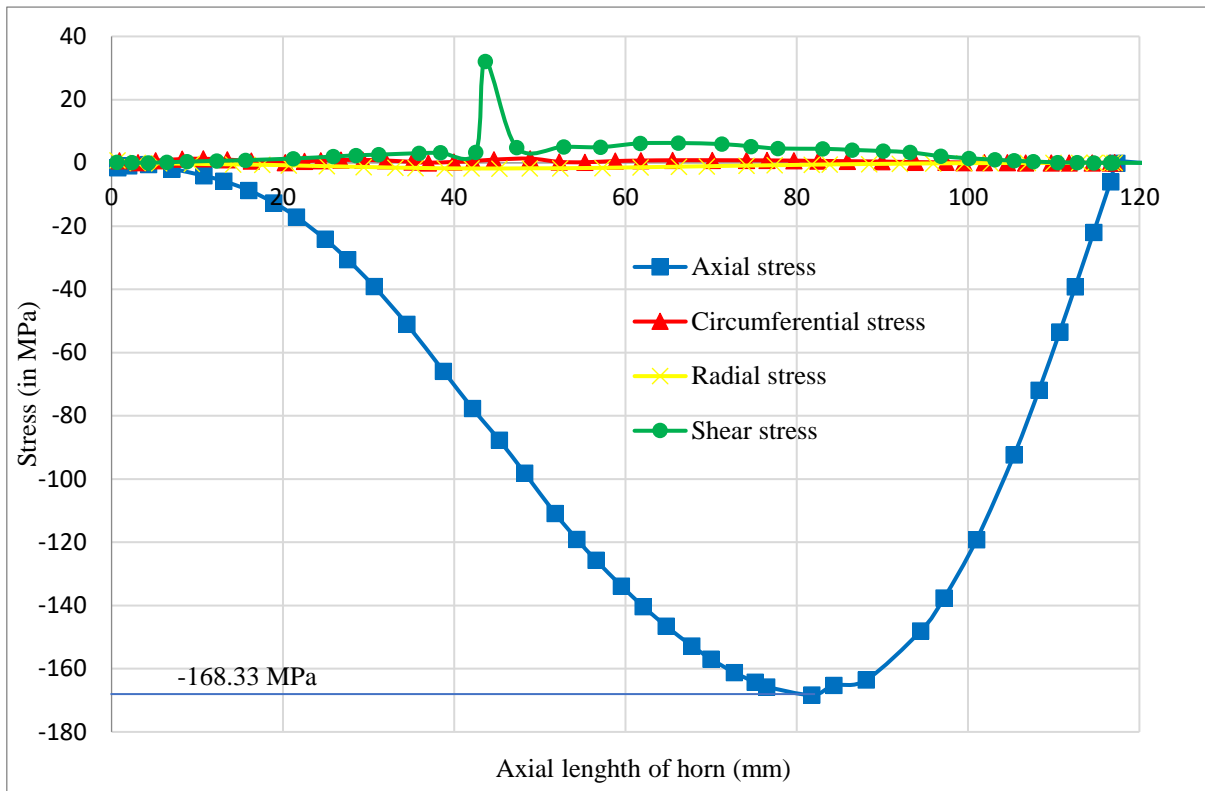


**Figure 11.** Stress variation along the axial length of titanium catenoidal horn

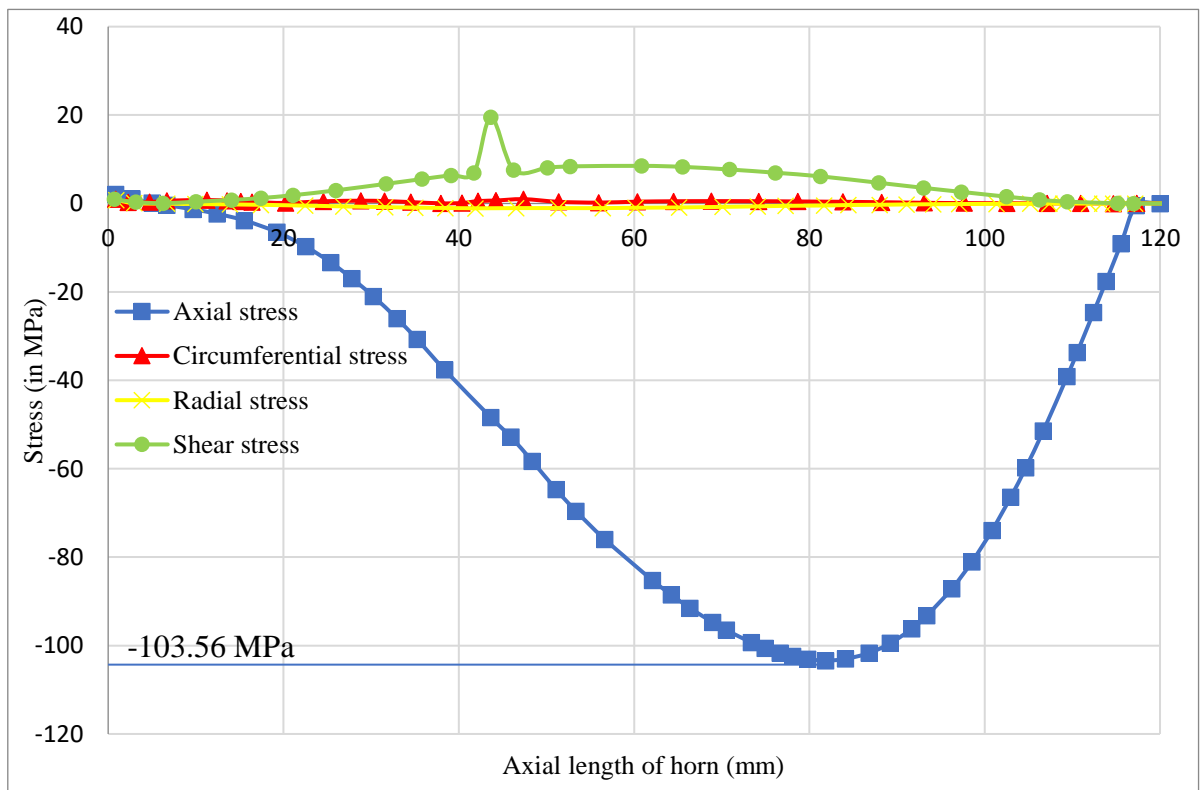


**Figure 12.** Stress variation along the axial length of aluminium catenoidal horn

## 5. Conclusions

Design and analysis of aluminum and titanium catenoidal horns with a circular hole at its tool end for USM by using modal and harmonic response module of ANSYS. Modal analysis was performed on horns for the determination of resonant frequency corresponding to axial mode shape. The results of the modal analysis reveals that the resonant frequency condition of achieving a frequency greater than 20 kHz for both horns can be achieved effectively for present horns designs. Harmonic analysis was also performed on the CAD models for the determination of MF and various stresses. Based on the harmonic analysis results an MF and equivalent stress of (5.32, 168.33 MPa for titanium) and (5.23, 103.56 MPa for aluminium) horns respectively can be achieved for present design. These results was compared with the available results of literature as tabulated in table 2. Results shows both horns have high MF as compared to existing horns this higher MF indicates better performance of the horn in USM with a high removal rate of material from the workpiece with low cutting force. Furthermore, stress magnitude in the axial direction of horns indicates that maximum stress developed has a magnitude of -103.56 MPa for aluminum and -168.33 MPa for titanium catenoidal horn but still this magnirude is less than the yield limit of material hence, lie within the acceptable range therefore horns are also safe against axial stress and can be used effectively in USM for machining of hard composite materials as a replacement of existing horn design. The same type of work for quadratic and cubic Bezier horn, 3<sup>rd</sup> order polynomial horn with steel, and Monel as their material can also be done and recommended as future work.

**Declaration of Competing Interest** The authors declare that they have no known competing interest.

## References

- [1] H. Zha, P. Feng, J. Zhang, D. Yu, and Z. J. T. I. J. o. A. M. T. Wu, "Material removal mechanism in rotary ultrasonic machining of high-volume fraction SiCp/Al composites," *The International Journal of Advanced Manufacturing Technology*, vol. 97, no. 5, pp. 2099-2109, 2018.
- [2] M. Sayuti, A. A. Sarhan, M. Fadzil, and M. J. T. I. J. o. A. M. T. Hamdi, "Enhancement and verification of a machined surface quality for glass milling operation using CBN grinding tool—Taguchi approach," *The International Journal of Advanced Manufacturing Technology*, vol. 60, no. 9, pp. 939-950, 2012.
- [3] Z.-P. Wan and Y. J. T. I. J. o. A. M. T. Tang, "Brittle–ductile mode cutting of glass based on controlling cracks initiation and propagation," *The International Journal of Advanced Manufacturing Technology*, vol. 43, no. 11, pp. 1051-1059, 2009.
- [4] J. Wang, C. Zhang, P. Feng, and J. J. T. I. J. o. A. M. T. Zhang, "A model for prediction of subsurface damage in rotary ultrasonic face milling of optical K9 glass," *The International Journal of Advanced Manufacturing Technology*, vol. 83, no. 1, pp. 347-355, 2016.

- [5] K. H. Mughal, M. A. M. Qureshi, S. F. J. E. T. Raza, and Innovation, "Novel ultrasonic horn design for machining advanced brittle composites: A step forward towards green and sustainable manufacturing," *Environmental Technology Innovation*, vol. 23, p. 101652, 2021.
- [6] K. Seah, Y. Wong, and L. J. J. o. M. P. T. Lee, "Design of tool holders for ultrasonic machining using FEM," *Journal of Materials Processing Technology*, vol. 37, no. 1-4, pp. 801-816, 1993.
- [7] S. Amin, M. Ahmed, and H. J. J. o. M. P. T. Youssef, "Computer-aided design of acoustic horns for ultrasonic machining using finite-element analysis," *Journal of Materials Processing Technology*, vol. 55, no. 3-4, pp. 254-260, 1995.
- [8] D.-A. Wang, W.-Y. Chuang, K. Hsu, and H.-T. J. U. Pham, "Design of a Bézier-profile horn for high displacement amplification," *Ultrasonics*, vol. 51, no. 2, pp. 148-156, 2011.
- [9] I.-C. Rosca, M.-I. Pop, and N. J. A. A. Cretu, "Experimental and numerical study on an ultrasonic horn with shape designed with an optimization algorithm," *Applied Acoustics*, vol. 95, pp. 60-69, 2015.
- [10] S. J. T. I. J. o. A. M. T. Roy, "Design of a circular hollow ultrasonic horn for USM using finite element analysis," *The International Journal of Advanced Manufacturing Technology*, vol. 93, no. 1, pp. 319-328, 2017.
- [11] A. J. J. o. t. B. S. o. M. S. Ray and Engineering, "Design and performance analysis of ultrasonic horn with a longitudinally changing rectangular cross section for USM using finite element analysis," *Journal of the Brazilian Society of Mechanical Sciences Engineering*, vol. 40, no. 7, pp. 1-11, 2018.
- [12] R. Naseri, K. Koohkan, M. Ebrahimi, F. Djavanroodi, and H. J. T. I. J. o. A. M. T. Ahmadian, "Horn design for ultrasonic vibration-aided equal channel angular pressing," *The International Journal of Advanced Manufacturing Technology*, vol. 90, no. 5, pp. 1727-1734, 2017.
- [13] M. R. Rani, K. Prakasan, and R. J. U. Rudramoorthy, "Studies on thermo-elastic heating of horns used in ultrasonic plastic welding," *Ultrasonics*, vol. 55, pp. 123-132, 2015.
- [14] J. Wang, Q. Sun, J. Teng, P. Jin, T. Zhang, and J. J. J. o. M. P. T. Feng, "Enhanced arc-acoustic interaction by stepped-plate radiator in ultrasonic wave-assisted GTAW," *Journal of Materials Processing Technology*, vol. 262, pp. 19-31, 2018.
- [15] P. K. Rai, V. Yadava, R. K. J. J. o. t. B. S. o. M. S. Patel, and Engineering, "Design of Bezier profile horns by using optimization for high amplification," vol. 42, no. 6, pp. 1-15, 2020.
- [16] I. C. Roşca, S. T. Chiriacescu, and N. C. J. P. P. Creţu, "Ultrasonic horns optimization," *Physics Procedia*, vol. 3, no. 1, pp. 1033-1040, 2010.
- [17] A. G. J. P. o. t. N. A. o. S. o. t. U. S. o. A. Webster, "Acoustical impedance and the theory of horns and of the phonograph," *Proceedings of the National Academy of Sciences of the United States of America*, vol. 5, no. 7, p. 275, 1919.
- [18] S. S. Rao, *Mechanical Vibrations*. Pearson Education, Incorporated, 2017.
- [19] A. P. Boresi, R. J. Schmidt, and O. M. Sidebottom, *Advanced mechanics of materials*. Wiley New York, 1985.
- [20] M. Nađ, "Ultrasonic horn design for ultrasonic machining technologies," *Applied and Computational Mechanics 4 (2010)* pp. 79-88, 2010.
- [21] M. R. Rani and R. J. U. Rudramoorthy, "Computational modeling and experimental studies of the dynamic performance of ultrasonic horn profiles used in plastic welding," *Ultrasonics*, vol. 53, no. 3, pp. 763-772, 2013.